Theoretical Analysis of Joint THP/pre-FDE For Single-carrier Signal Transmissions

Kazuki TAKEDA[†] Hiromichi TOMEBA[†] and Fumiyuki ADACHI[‡]
Dept. of Electrical and Communication Engineering, Graduate School of Engineering, Tohoku University
6-6-05, Aza-Aoba, Aramaki, Aoba-ku, Sendai, 980-8579 JAPAN
[†]{kazuki, tomeba}@mobile.ecei.tohoku.ac.jp, [‡]adachi@ecei.tohoku.ac.jp

***Abstract*—Frequency-domain pre-equalization (pre-FDE) can improve the single-carrier (SC) signal transmission performance in a severe frequency-selective channel. However, the performance improvement is limited by the residual inter-symbol interference (ISI). The residual ISI can be eliminated by the joint use of Tomlinson-Harashima precoding and frequency-domain pre-equalization (called joint THP/pre-FDE) and its performance improvement was confirmed by computer simulation in [8]. In this paper, we present a theoretical analysis of joint THP/pre-FDE. The conditional bit error rate (BER) for the given channel realization is derived by taking into account the modulo operation error in a receiver and the achievable BER performance is numerically evaluated.**

Keywords-components; Pre-equalization, Tomlinson-Harashima precoding, single-carrier

I. INTRODUCTION

Broadband single-carrier (SC) signal transmission performance significantly degrades due to a strong inter-symbol interference (ISI) resulting from a severe frequency-selective fading channel [1]. Frequency-domain equalization (FDE) based on the minimum mean square error (MMSE) criterion improves the bit error rate (BER) performance [2, 3]. However, the performance improvement is limited by the presence of the residual ISI after FDE [4]. Recently, we proposed a joint use of Tomlinson-Harashima precoding (THP) [5, 6] and FDE, called joint THP/FDE, to eliminate the residual ISI [7]. Assuming the perfect channel state information (CSI), joint THP/FDE can remove the residual ISI completely.

The use of joint THP/FDE requires the CSI and computational expensive signal processing at both a transmitter and a receiver. We proposed a joint use of THP and frequency-domain pre-equalization (pre-FDE), called joint THP/pre-FDE [8]. Joint THP/pre-FDE offers almost the same BER performance as the joint THP/FDE while simplifying the receivers (no CSI and equalization are required at receivers). The performance of joint THP/pre-FDE was evaluated by computer simulation only [8].

In this paper, we present a theoretical analysis of joint THP/pre-FDE. The remainder of this paper is organized as follows. Section II reviews the joint THP/pre-FDE. In Sec. III, the conditional BER for the given channel realization is derived by taking into account the modulo operation error in a receiver. The BER performance is evaluated by Monte-Carlo numerical computation method and compared with the computer simulation result in Sec. IV. Sec. V concludes this paper.

II. JOINT THP/PRE-FDE

In this paper, we use a symbol-spaced discrete time signal representation. We assume the perfect CSI.

A. Channel model

The channel is assumed to be an L-path frequency-selective block fading channel having the impulse response given as

$$h(\tau)=\sum_{l=0}^{L-1}h_l\delta(\tau-\tau_l)\,, \tag{1}$$

where h_l and τ_l represent the complex-valued path gain with $\sum_{l=0}^{L-1}E[|h_l|^2]=1$ and the time delay of the l-th path, respectively.

B. Transmit Signal

Figure 1 illustrates the transmitter structure of joint THP/pre-FDE. A block transmission of N_c symbols is considered. At first, the data symbol vector $\mathbf{s}=[s(0), \ldots, s(t), \ldots, s(N_c-1)]^T$ is input to the THP block whose structure is depicted in Fig. 2. Modulo operator [9] is used to avoid the amplitude increase in the THP output signal. Figure 3 shows the modulo operator input-output relationship. The modulo operator output can be expressed as

$$Output=Input+2Mz\,, \tag{2}$$

where $2Mz$ represents the modulo operation. The real and imaginary parts of z are respectively an integer so that they are limited within an interval $[-M, M)$.

Letting $\mathbf{B}$ be the feedback matrix characterized by an $N_c\times N_c$ lower triangular matrix, the THP output signal vector $\mathbf{y}=[y(0), \ldots, y(t), \ldots, y(N_c-1)]^T$ can be expressed as

$$\begin{aligned}\mathbf{y}&=\Omega(\mathbf{h})\cdot\{diag(\mathbf{B})\}^{-1}\{\mathbf{s}-(\mathbf{B}-diag(\mathbf{B}))\left(\mathbf{y}/\Omega(\mathbf{h})\right)+2M\mathbf{z}_t\}\\&=\Omega(\mathbf{h})\cdot\mathbf{B}^{-1}\cdot\left(\mathbf{s}+2M\mathbf{z}_t\right)\end{aligned}\ , \tag{3}$$

where $\Omega(\mathbf{h})$ denotes the power normalization coefficient to keep the average transmit power the same before and after THP and $2M\mathbf{z}_t=[2Mz_t(0), \ldots, 2Mz_t(t), \ldots, 2Mz_t(N_c-1)]^T$. $\mathbf{B}$ and $\Omega(\mathbf{h})$ are given by

$$\begin{cases} \mathbf{B} = \begin{bmatrix} B_{0,0} & & \mathbf{0} \\ \vdots & \ddots & \\ B_{N_c-1,0} & \cdots & B_{N_c-1,N_c-1} \end{bmatrix} \\ \Omega(\mathbf{h}) = \sqrt{N_c / \sum_{\tau=0}^{N_c-1} (1/|B_{\tau,\tau}|^2)} \end{cases} . \tag{4}$$

The input signal vector $\mathbf{x}=[x(0), \ldots, x(t), \ldots, x(N_c-1)]^T$ to pre-FDE is obtained as

$$\mathbf{x} = \mathbf{G}\mathbf{y} , \tag{5}$$

where $\mathbf{G}$ is an $N_c \times N_c$ unitary matrix ($\mathbf{G}$ is shown later). $\mathbf{x}$ is transformed by using an N_c-point fast Fourier transform (FFT) into the frequency-domain signal to carry out the pre-FDE. The pre-equalized frequency-domain signal is transformed back to the time-domain signal vector $\mathbf{x}$' by using an N_c-point inverse FFT (IFFT). After inserting the cyclic prefix (CP) into the guard interval (GI), the signal block is transmitted.

C. Received Signal

The concatenation of the pre-FDE and the propagation channel can be regarded as the equivalent channel, given by

$$\hat{H}(k) = W(k)H(k) , \tag{6}$$

where $H(k)$ represents the propagation channel gain given as

$$H(k) = \sum_{l=0}^{L-1} h_l \exp\left(-j2\pi k \frac{\tau_l}{N_c}\right) \tag{7}$$

and $W(k)$ is the pre-FDE weight. In this paper, we use pre-FDE weight based on the equal gain (EG) criterion, which is given as

$$W(k) = \frac{H^*(k)}{|H(k)|} . \tag{8}$$

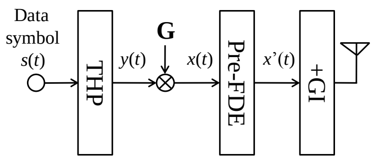

Fig. 1 Transmitter.

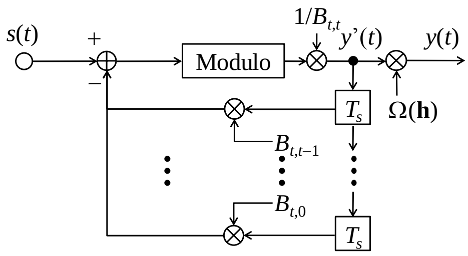

Fig. 2 THP.

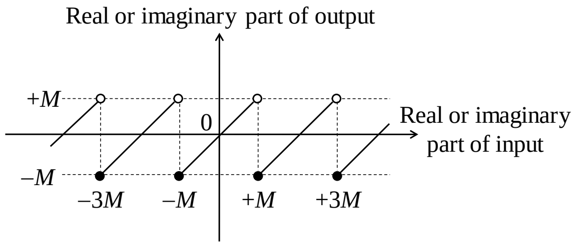

Fig. 3 Input-output relationship of modulo operator.

The received signal vector $\mathbf{r}=[r(0), \ldots, r(t), \ldots, r(N_c-1)]^T$ after removing the GI can be expressed as

$$\mathbf{r} = \sqrt{\frac{2E_s}{T_s}} \hat{\mathbf{h}}\mathbf{x} + \mathbf{n} , \tag{9}$$

where E_s and T_s are the average transmit symbol energy and the symbol duration, respectively, and $\mathbf{n}=[n(0), \ldots, n(t), \ldots, n(N_c-1)]^T$ is the noise vector, whose elements are independent complex Gaussian variables with zero-mean and variance $2N_0/T_s$. N_0 is the one-sided power spectrum density of the additive white Gaussian noise (AWGN). $\hat{\mathbf{h}}$ is an $N_c \times N_c$ impulse response matrix of the equivalent channel and is given as [8]

$$\hat{\mathbf{h}} = \begin{bmatrix} \hat{h}_0 & \hat{h}_{N_c-1} & & \hat{h}_2 & \hat{h}_1 \\ \hat{h}_1 & \hat{h}_0 & \ddots & \vdots & \hat{h}_2 \\ \hat{h}_2 & \hat{h}_1 & \ddots & \hat{h}_{N_c-1} & \vdots \\ \vdots & \hat{h}_2 & \ddots & \hat{h}_0 & \hat{h}_{N_c-1} \\ \hat{h}_{N_c-1} & \vdots & & \hat{h}_1 & \hat{h}_0 \end{bmatrix} \tag{10}$$

with

$$\hat{h}_l = \frac{1}{N_c} \sum_{k=0}^{N_c-1} W(k)H(k) \exp\left(j2\pi k \frac{l}{N_c}\right). \tag{11}$$

By applying the LQ-decomposition [10] to the equivalent channel matrix as $\hat{\mathbf{h}} = \mathbf{LQ}$ and setting $\mathbf{G}=\mathbf{Q}^H$ and $\mathbf{B}=\mathbf{L}$, Eq. (9) can be rewritten as

$$\mathbf{r} = \sqrt{\frac{2E_s}{T_s}}\mathbf{LQx} + \mathbf{n} = \sqrt{\frac{2E_s}{T_s}}\Omega(\mathbf{h}) \cdot (\mathbf{s} + 2M\mathbf{z}_t) + \mathbf{n} . \qquad (12)$$

Figure 4 illustrates the received signal constellation of **r**. At the receiver, the decision variable vector $\hat{\mathbf{s}} = [\hat{s}(0), \ldots, \hat{s}(t), \ldots, \hat{s}(N_c-1)]^T$ can be obtained only by applying the modulo operation as

$$\begin{aligned} \hat{\mathbf{s}} &= \left(\sqrt{\frac{2E_s}{T_s}}\Omega(\mathbf{h}) \right)^{-1} \mathbf{r} - 2M\mathbf{z}_r \\ &= \mathbf{s} + 2M(\mathbf{z}_t - \mathbf{z}_r) + \left(\sqrt{\frac{2E_s}{T_s}}\Omega(\mathbf{h}) \right)^{-1} \mathbf{n} \end{aligned} , \qquad (13)$$

where $-2M\mathbf{z}_r = [-2Mz_r(0), \ldots, -2Mz_r(t), \ldots, -2Mz_r(N_c-1)]^T$ represents the modulo operation at the receiver.

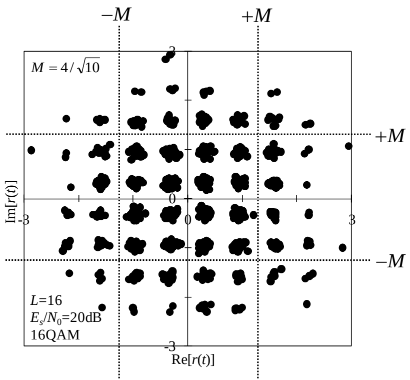

Fig. 4 Signal constellation of **r**.

III. Theoretical BER Analysis

We first derive the approximate conditional BER expression and obtain the optimal modulo operation size *M*. We assume QPSK and 16 QAM.

A. Conditional BER

In the receiver, the data decision is made by removing $2M\mathbf{z}_t$ and applying the modulo operation. A combination of the most probable transmitted symbol $\hat{s}(t)$ and the modulo operation $2Mz_r(t)$ is searched as

$$\left(\hat{s}(t), 2Mz_r(t)\right) = \min_{\substack{\hat{s}(t)\in\boldsymbol{\Theta} \\ \mathrm{Re}[z_r(t)]\in\mathbf{Z} \\ \mathrm{Im}[z_r(t)]\in\mathbf{Z}}} \left\| \begin{matrix} \{s(t) - \hat{s}(t)\} + 2M\{z_t(t) - z_r(t)\} \\ + \left(\sqrt{\frac{2E_s}{T_s}}\Omega(\mathbf{h}) \right)^{-1} n(t) \end{matrix} \right\| , \qquad (14)$$

where $\boldsymbol{\Theta}$ is a set of data symbol candidates and **Z** is a set of all integers.

The Gray code mapping is used for data modulation. For simplifying the analysis, it is assumed that only one bit error in the transmitted symbol is produced. The decision error occurs when $\hat{s}(t) \neq s(t)$ or $2Mz_r(t) \neq 2Mz_t(t)$. In this case, the bit error probability can be approximated as

$$\begin{aligned} &\mathrm{Prob}\{\hat{s}(t) \neq s(t) \cup 2Mz_r(t) \neq 2Mz_t(t)\} \\ &\quad \approx \mathrm{Prob}\{\hat{s}(t) \neq s(t)\} + \mathrm{Prob}\{2Mz_r(t) \neq 2Mz_t(t)\} \end{aligned} . \qquad (15)$$

The first term of Eq. (15) is the probability that the received signal falls outside the symbol decision boundary under the condition that the received signal is inside the modulo operation boundary of $\pm M$. This probability is approximately given for QPSK and 16QAM as

$$\mathrm{Prob}\{\hat{s}(t) \neq s(t)\} \approx \begin{cases} \frac{1}{2} erfc\left(\sqrt{\frac{\gamma}{4}}\right) & \text{for QPSK} \\ \frac{3}{8} erfc\left(\sqrt{\frac{\gamma}{20}}\right) & \text{for 16QAM} \end{cases} , \qquad (16)$$

where γ is the conditional signal-to-noise power ratio (SNR) and $erfc(x) = 2/\sqrt{\pi}\int_x^\infty \exp(-t^2)dt$ is the complementary error function. The second term of Eq. (15) is the probability that the received signal falls outside the modulo operation boundary (note that this modulo operation error produces 1 bit error per symbol only). $\mathrm{Prob}\{2Mz_r(t) \neq 2Mz_t(t)\}$ is derived below.

The decision error event, i.e., $2Mz_r(t) \neq 2Mz_t(t)$, is produced by the modulo operation error. This happens when the received signal falls outside the modulo operation boundary of $\pm M$. This error event happens most likely when the signal nearest the modulo operation boundary (and hence the outermost) is transmitted. Figure 5 illustrates the real part of the signal constellation. Since the shortest distance between the modulo boundary and the outermost signal is $(M - 1/\sqrt{2})$ for QPSK and $(M - 3/\sqrt{10})$ for 16QAM, we have

$$\mathrm{Prob}\{2Mz_r(t) \neq 2Mz_t(t)\} \approx \begin{cases} \frac{1}{2} \cdot erfc\left(\sqrt{\frac{\gamma}{2}}(M - \frac{1}{\sqrt{2}})\right) & \text{for QPSK} \\ \frac{1}{4} \cdot erfc\left(\sqrt{\frac{\gamma}{2}}(M - \frac{3}{\sqrt{10}})\right) & \text{for 16QAM} \end{cases} . \qquad (17)$$

From Eqs. (15)~(17), the conditional BER for the given γ and *M* can be obtained as

$$p_b(M,\gamma) \approx \begin{cases} \frac{1}{2}\cdot erfc\left(\sqrt{\frac{\gamma}{4}}\right) \\ +\frac{1}{2}\cdot erfc\left(\sqrt{\frac{\gamma}{2}}(M-\frac{1}{\sqrt{2}})\right) \text{ for QPSK} \\ \frac{3}{8}\cdot erfc\left(\sqrt{\frac{\gamma}{20}}\right) \\ +\frac{1}{4}\cdot erfc\left(\sqrt{\frac{\gamma}{2}}(M-\frac{3}{\sqrt{10}})\right) \text{ for 16QAM} \end{cases} . \quad (18)$$

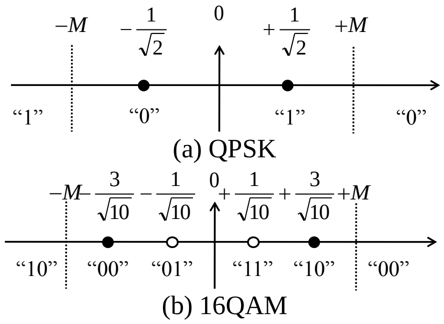

Fig. 5 Real part of the signal constellation.

B. Received SNR

The received SNR γ for the given channel condition **h** is obtained from Eq. (13) as

$$\gamma = \frac{2E_s}{N_0}\{\Omega(\mathbf{h})\}^2 . \quad (19)$$

The transmit signal at the modulo operator output is uniformly distributed in a square area of $-M \le \{\text{Real, Imaginary}\} < M$ in a strong frequency-selective channel environment. Therefore, the average transmit symbol energy E_s is given as

$$E_s = \frac{3}{2M^2}\left\{N \cdot E_b \cdot \frac{N_c}{N_c+N_g}\right\}, \quad (20)$$

where E_b and N denote the average transmit bit energy and the number of bits per symbol, respectively. From Eqs. (19) and (20), we have

$$\gamma = \frac{N}{M^2}\cdot\frac{3\{\Omega(\mathbf{h})\}^2}{1+N_g/N_c}\cdot\frac{E_b}{N_0} . \quad (21)$$

The average BER can be numerically evaluated by averaging Eq. (18) over all possible realizations of channel **h**.

C. Optimal M

As the modulo operation size *M* increases, the first term of Eq. (18) increases while the second term of Eq. (18) decreases. As a consequence, there exists the optimal *M* that minimizes the conditional BER. Using

$$\frac{\partial}{\partial x}erfc(x) = -\frac{2}{\sqrt{\pi}}\exp(-x^2) \quad (22)$$

and solving $\partial p_b(M,\gamma)/\partial M = 0$, the optimal *M* can be derived as (the derivation is omitted for the sake of brevity)

$$M_{opt} = \begin{cases} \sqrt{2} & \text{for QPSK} \\ \dfrac{3\sqrt{10} + \sqrt{10 + 8\left(\frac{1}{5}\frac{E_b}{N_0}\frac{3\Omega^2(\mathbf{h})}{1+N_g/N_c}\right)^{-1}\ln 2}}{10 - \left(\frac{1}{5}\frac{E_b}{N_0}\frac{3\Omega^2(\mathbf{h})}{1+N_g/N_c}\right)^{-1}\ln 2} & \text{for 16QAM} \end{cases} . \quad (23)$$

In [5]-[8], *M* is chosen so that $\{s(t)+2Mz_t(t)\}$ is equidistantly distributed over (*I*, *Q*)-plane; $M=\sqrt{2}$ for QPSK and $M=4/\sqrt{10}$ for 16QAM. However, $M=4/\sqrt{10}$ for 16QAM is not optimal in the sense of minimum BER.

IV. NUMERICAL COMPUTATION

Table 1 summarizes the numerical computation and computer simulation parameters. We assume an L=16-path frequency-selective block Rayleigh fading channel having exponential power delay profile with the decay factor α dB.

Table 1 Numerical and simulation condition

Transmitter	Data modulation	QPSK, 16QAM
	No. of FFT points	N_c=128
	GI length	N_g=16
	FDE	EGC
Channel estimation		Perfect
Channel	Frequency-selective block Rayleigh	
	Power delay profile shape	L=16 exponential power delay profile
	Decay factor	α=0, 6dB
	Delay time	$\tau_l=l$, l=0~L−1

Figure 6 shows the optimal *M* given by Eq. (23) as a function of E_b/N_0 for QPSK and 16QAM when $\Omega^2(\mathbf{h})=1$. For QPSK, since the probability of modulo operation error is the same for all transmitted symbols, the optimal *M* is the same as the equidistant constellation case (i.e., $M=\sqrt{2}$). On the other hand, for 16QAM, the outermost signals in the constellation are most likely to be in modulo operation error (see Fig. 5).

Therefore, in order to minimize the modulo operation error probability in a low E_b/N_0 region, the optimal M becomes larger than for the equidistant signal constellation case (i.e., $M = 4/\sqrt{10}$). In a high E_b/N_0 region, to reduce the transmit signal power increase, the optimal M approaches the case of the equidistant signal constellation (i.e., $M = 4/\sqrt{10}$).

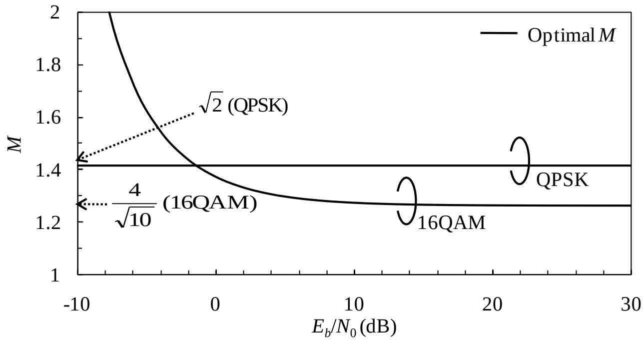

Fig. 6 Optimal M.

Figure 7 plots the numerically evaluated average BER performances for QPSK and 16QAM when α=0dB (uniform power delay profile). When QPSK is used, the optimal M is the same as the equidistant constellation case and hence, the same BER performance is achieved. When 16QAM is used, the optimal M is larger than the equidistant constellation case in a very low E_b/N_0 region (see Fig. 6), however the achievable BER performance is almost the same as in the equidistant case. Therefore, the constant M can be used.

Figure 8 compares the numerically evaluated BER performance and the computer simulated BER performance. The constant M is used (i.e., $M = \sqrt{2}$ for QPSK and $M = 4/\sqrt{10}$ for 16QAM). A fairly good agreement is seen between the numerical and simulated BER performances. This confirms the validity of our conditional BER analysis.

V. CONCLUSION

In this paper, we presented a theoretical analysis of joint THP/pre-FDE. The conditional BER for the given channel condition was derived by taking into account the modulo operation error at the receiver. The optimal modulo operation size M was derived based on the minimum BER criterion. The achievable BER performance was numerically evaluated by Monte-Carlo numerical computation method. The numerical computed BER performance was confirmed by computer simulation.

REFERENCES

[1] W. C. Jakes Jr., ed., *Microwave Mobile Communications*, Wiley, New York, 1974.

[2] D. Falconer, S. L. Ariyavisitakul, A. Benyamin-Seeyar and B. Eidson, “Frequency domain equalization for single-carrier broadband wireless systems,” IEEE Commun., Mag., Vol. 40, No. 4, pp. 58-66, Apr. 2002.

[3] F. Adachi, D. Garg, S. Takaoka, and Kazuaki Takeda, “Broadband CDMA techniques,” IEEE Wireless Commun. Mag., Vol. 12, No. 2, pp. 8-18, April 2005.

[4] Kazuaki Takeda and F. Adachi, “Bit error rate analysis of DS-CDMA with joint frequency-domain equalization and antenna diversity reception,” IEICE Trans. Commun., Vol. E87-B, No. 10, pp. 2991-3002, Oct. 2004.

[5] M. Tomlinson, “New automatic equalizer employing modulo arithmetic,” Electronics Letters, Vol. 7, No. 5/6, pp. 138-139, Mar. 1971.

[6] H. Harashima and H. Miyakawa, “Matched-transmission technique for channels with intersymbol interference,” IEEE Trans. Commun., Vol. 20, No. 4, pp. 774-780, Aug. 1972.

[7] Kazuki Takeda, H. Tomeba and F. Adachi, “Joint Tomlinson-Harashima precoding and frequency-domain equalization for broadband single-carrier transmission,” IEICE Trans. Commun., Vol. E91-B No. 1, pp.258-266, Jan. 2008.

[8] Kazuki Takeda, H. Tomeba and F. Adachi, “BER performance of joint THP/pre-FDE,” Proc. IEEE 67th Veh. Technol. Conf., pp. 1016-1020, May 2008.

[9] R. Fischer, “The modulo-lattice channel: the key feature in precoding schemes,” Inter. J. of Elec. and Commun., Vol. 59, No. 4, pp. 244-253, Jun. 2005.

[10] G. H. Golub and C. F. Van Loan, *Matrix Computations*, 2nd Edition, The Johns Hopkins University Press, 1989.

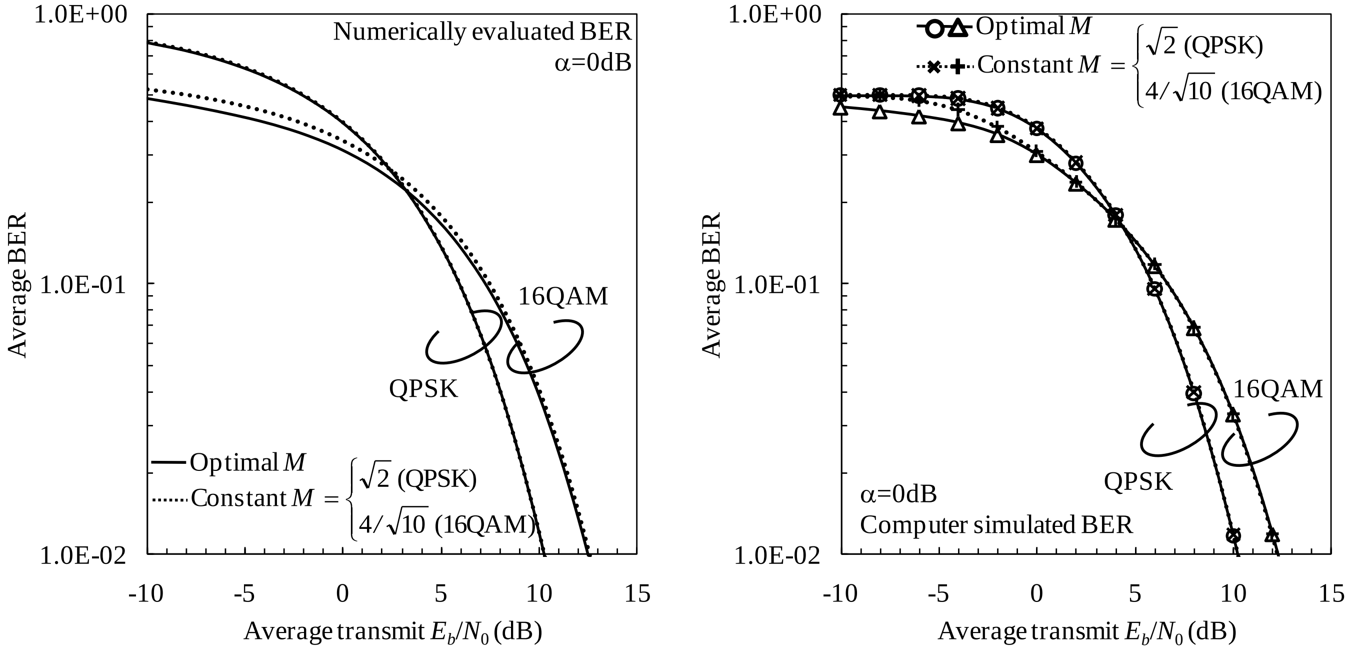

(a) Numerical (b) Simulation

Fig. 7 Average BER performance comparison between the optimal M and the constant M.

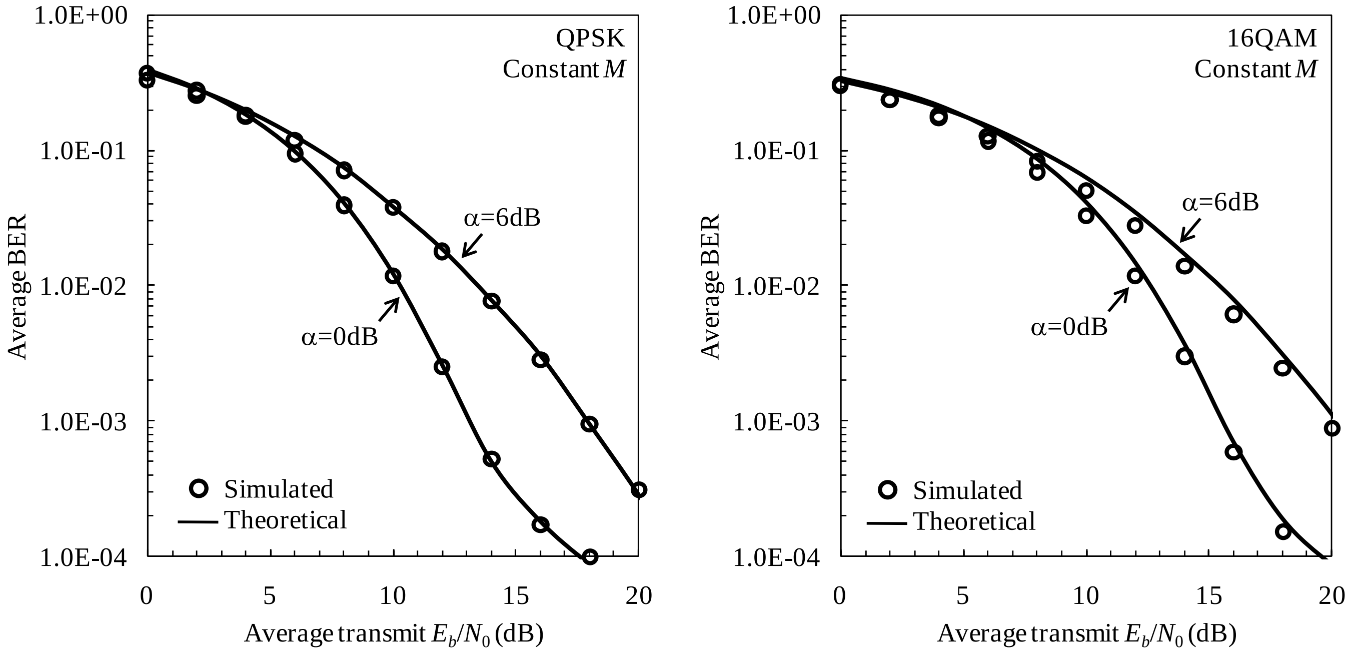

(a) QPSK (b) 16QAM

Fig. 8 Performance comparison between the numerically evaluated BER and the computer simulated BER.